An improved aerothermal database for hypervelocity air flows up to 25 km/s

Gabriela Almeida Gomes
gabriela.a.gomes@tecnico.ulisboa.pt

Instituto Superior Técnico, Universidade de Lisboa, Portugal

July 2022

Abstract

For hypervelocity flows above 10 km/s, the strong bow-shock wave converts the flow coherent energy into thermal agitation energy. Most of this energy is then transferred into the gas species internal modes or consumed through endothermic processes. Simulating higher velocities contributes to the understanding of hypersonic high-temperature flows and paves the way for these velocities to be considered for Space missions. This work aims to simulate extreme velocities using the SPARK CFD code, by including the necessary enhancements to its aerothermal database. For a ram pressure of 0.1 MPa, the simulations were typically limited to velocities lower than 14 km/s, as the thermodynamic properties used were fitted only up to 20 000 K. Accordingly, these have been updated, extending their validity to 100 000 K. Atomic and molecular species internal levels spectroscopic data was compiled, with reconstruction of molecular potential curves and determination of the corresponding rovibronic levels. Partition functions were calculated and the determined thermodynamic properties were compared to other databases, validating the implementation. The impact of adding double and triple ionization for atoms was evaluated. For velocities higher than 18 km/s, single ionization is capped and double is required, as it becomes an important energy loss term, significantly decreasing the temperatures at the shock layer. Velocities up to 25 km/s were simulated, with triple ionization found to not impact the flowfield significantly, as double ionization is not yet capped. Nevertheless, its inclusion is recommended, as it increases the simulations' fidelity and might become necessary for higher velocities.
Keywords: Hypersonic, Aerothermodynamics, Kinetics, Air Properties, Meteoroids

1. Introduction

Hypersonic high-temperature flows entail a variety of phenomena that need to be carefully studied and modeled, encapsulating many areas of knowledge that interact with one another. Typical studies in this field are applied to spacecraft re-entry velocities; besides the usual phenomena studied in those cases, additional processes have to be considered when studying even higher velocities, such as those reached by meteoroids.

This work will focus on some of the enhancements necessary to simulate high velocity flows previously never reached using the SPARK CFD code. Higher velocities will activate increasingly important energy loss terms such as the endothermic chemistry reactions, therefore those need to be modeled; the extension of thermodynamic properties database for higher ranges of temperatures is also necessary for accurate simulations.

We have modeled hypersonic high-temperature flows for a gas mixture of 15 species (N_2, O_2, NO, N_2^+, O_2^+, NO^+, N, O, N^+, O^+, N^{++}, O^{++}, N^{+++}, O^{+++}, e^-), in the continuum regime, around spherical meteoroids with 0.3 m radius, subject to ram pressure of 0.1 MPa, for velocities in the range 8 - 25 km/s.

While the principles studied in the following chapters and the reached conclusions are mostly theoretical, these may be applied to various cases of hypersonic high-temperature flows. The example of meteoroids entering Earth's atmosphere will accompany us for the entirety of this work, for the following reasons: they represent, nowadays, the objects that enter our atmosphere at higher velocities, with values that may theoretically vary from 11 to 72 km/s - the mean velocity values of the observed meteoroids are between 25 and 30 km/s, speeds more in line with Near-Earth Objects; the assumed spherical shape simplifies grid adaptation and flowfield convergence stability [12] and creates a detached bow shock similar to what happens with blunt-body spacecrafts, therefore some conclusions are applicable to those studies; Earth's atmosphere has up to date data, being useful for the studies

here performed and, on the other hand, the application to our planet's example in the elaboration of databases, thermodynamic models and kinetic models makes them particularly relevant; studies on these hypersonic high-temperature flows contribute to risk assessment of meteoroid's events.

2. Atmospheric Entry Hypersonic Flows

Hypersonic flows are generally characterized by the presence of compressibility effects leading to the formation of strong and high temperature shock waves. Tipically, freestream flows with a Mach number higher than 5 are said to be in the hypersonic regime; however for the velocities here considered, the flow is chemically reacting and the definition of Mach number loses some significance and it is more common to think in terms of velocities [1].

The dynamics associated with this flight regime are very different from those considered in subsonic or even supersonic flows. Picturing a spherical meteoroid in the hypersonic regime, it creates a detached bow shock wave. In the shock layer the flow is quickly decelerated until the stagnation point through the transfer of kinetic to thermal energy. As a result, extreme temperatures are reached - in the $10^4 - 10^5$ K range - and the so-called high-temperatures effects become important and have to be considered in the equations describing the flow. These physical-chemical phenomena include the endothermic reactions of dissociation and ionization (simple, double, ...) of chemical species - forming a plasma -, non-equilibrium thermochemistry (owing it to the high temperatures and the rarefied freestream flow) and radiative absorption and/or emission, as a result of excitation and de-excitation of the species internal degrees of freedom.

Laminar flow is typically assumed in the forebody region, due to the small Reynolds number in the stagnation region and to the strong favorable pressure conditions that will delay the transition to a turbulent flow. For the altitudes of interest of this work, the atmospheric density conditions are those of continuous flow therefore it may be modeled by finite volume methods and the Navier-Stokes equations.

In conclusion, the simulation of an atmospheric entry with computational fluid dynamics should consider all the phenomena described above. Although the interdependence between them is strong, the extremely high computational costs of simulations will compel the assumption of some decoupling between areas of study and even neglecting of some effects such as thermal non-equilibrium, in some cases.

3. State of the Art

Meteoroid science is a highly complex and polyvalent field, entailing problems from various areas of knowledge. Although some of its sub-disciplines are already well comprehended by scientists, shock waves in meteoroids are still a largely unknown phenomenon, with many prevalent questions remaining unanswered. The work of [24] resumes the main accomplishments in the area of meteor generated shock waves so far, balancing them with a review of the related hypersonic gas dynamics topics, as well as the questions scientists are still focusing on.

Aerothermodynamic modelling of the flow around a body is essential to this work. Depending on the flow regime encountered - described by the Knudsen number - different modelling methods must be employed. For bodies in the transitional and free molecular regimes, the Navier-Stokes equations are no longer valid and it is necessary to implement the Boltzmann equation of kinetic energy; direct simulation Monte Carlo (DSMC) [3] is the most commonly used method. Our work does not deal with rarefied regimes or such small meteoroids, operating in the continuum regime.

Fragmentation and ablation are two important phenomena that have had many studies performed on them, as they impact meteoroid's trajectory and behaviour, flow composition and the consequences on Earth. This work will focus on the theory and simulation of hypersonic high-temperature flow around a single non-ablating body, so these two topics will not be covered but are important to keep in mind for future applications to real meteoroid's events, in which these processes will be of great importance. [24, 5, 23] are examples of works that study these phenomena.

Entry shock wave studies are more prevalent in the area of reentry vehicles, where simulations and experiments have been made throughout the years for the planning of Space missions. The considered velocities are significantly lower than those that meteoroids may reach, with little cross disciplinary work having been made among meteoroid and shock wave investigators, mainly for velocities higher than 15km/s. However, [10] is a relevant exception: this work, applied to reentry vehicles, pushes the aerothermodynamic modelling capabilities forward, allowing for simulation of velocities from 16 km/s up to 22 km/s, while remaining in the continuum regime and using Navier-Stokes equations. It focuses on enhancements required to treat temperatures higher than 20 000 K (up to 50 000 K), such as thermodynamic properties suited to higher temperatures for atomic species, ionization potential lowering, addition of N^{++} and O^{++} and non-Boltzmann radiation modelling of N^{+}. The enhancements are applied to the LAURA/HARA coupled flowfield and radiation solver. The influence of coupled radiation and ablation in the simulations is also studied. This work will often be used to draw

comparisons to the work developed here, regarding some of the employed enhancements.

As for the determination of thermodynamic properties, level energies have to be determined and for diatomic molecules this may be done through the reconstruction of potential curves. Examples of works that make use of such methods are [17, 18, 19, 25].

Following [10], two other works by Johnston applied these developments to meteoroids. [14] used chemically reacting computational fluid dynamics, coupled with radiation transport and surface ablation, allowing the assessment of the heat transfer coefficient, commonly assumed as 0.1. Johnston [12] developed a model for simulating the radiative flux reaching the ground originating from a meteor shock-layer and wake, applying the methods developed in [10, 14] and using the Tunguska event as a test case - the largest meteor airburst event on Earth's recorded history. The work simulated ground heating footprints to assess entry parameters such as optimal initial radii.

In [6], radiation in hypersonic high-temperature flows is studied, using the SPARK Line-by-Line code - a radiative solver that computes the spectrally-dependent emission and absorption coefficients of a gas mixture in non-equilibrium and relies on results from the SPARK CFD solver. Loosely-coupled radiation simulation is yet to be implemented in the SPARK CFD code, as well as coupled radiation that would lead to more physically accurate simulation results and is something to strive for in the future of SPARK simulations. This work will not cover the effects of radiation in the shock layer.

4. Flowfield Modeling and Enhancements

SPARK (Software Package for Aerothermodynamics, Radiation and Kinetics) is the CFD code used throughout this work [20]. This flexible and extendable code simulates high-entropy hypersonic non-equilibrium flow.

To do so the macroscopic properties of the flow around the spherical meteoroid need to be determined, through the Navier-Stokes equations:

$$\frac{\partial(\rho c_s)}{\partial t} + \boldsymbol{\nabla}\cdot(\rho c_s \boldsymbol{V}) = \boldsymbol{\nabla}\cdot\boldsymbol{J_s} + \dot{w}_s \tag{1}$$

$$\frac{\partial(\rho \boldsymbol{V})}{\partial t} + \boldsymbol{\nabla}\cdot(\rho \boldsymbol{V}\otimes\boldsymbol{V}) = \boldsymbol{\nabla}\cdot[\boldsymbol{\tau}] - \boldsymbol{\nabla}p \tag{2}$$

$$\frac{\partial(\rho e)}{\partial t} + \boldsymbol{\nabla}\cdot(\rho \boldsymbol{V} e) = \boldsymbol{\nabla}\cdot(\boldsymbol{V}\cdot[\boldsymbol{\tau}]) - \boldsymbol{\nabla}\cdot(p\boldsymbol{V}) - \boldsymbol{\nabla}\cdot\boldsymbol{q} \tag{3}$$

where heat flux vector $\boldsymbol{q}$ is the sum of convective heat, diffusive heat and, in cases where radiation is considered, radiative heat:

$$\boldsymbol{q} = \sum_s \boldsymbol{J_s} h_s - \sum_k \kappa_k \boldsymbol{\nabla} T_k + \boldsymbol{q}_R \tag{4}$$

If multi-temperature models were to be used, for each non-equilibrium thermal mode there would be an additional equation, as each independent thermal mode's energy must be conserved. However, in this work a single-temperature model will be used, as the post-shock pressure will be high, leading to, on a first basis, a fast equilibrium of the different temperatures shortly after the shock.

4.1. Thermodynamic Properties

The determination of thermodynamic properties, such as entropy, enthalpy and internal energy, is key for the solving of the Navier-Stokes equations at high temperatures. In other words, to understand the thermodynamic tendencies of a high-temperature non-equilibrium reactive gas, a model that considers the species' internal structure is required - a quantum perspective of the problem is hence in order.

To do so, statistical thermodynamics is used - this theory views a gas as a collection of particles where each carries energy while moving through the flow. This energy is separated in the following energy modes: translational, rotational, vibrational and electronic. By the Born-Oppenheimer approximation, separation of different energy modes under simple circumstances is allowed. Therefore the contribution of different energy modes may be separated and the total internal energy of a single species per unit of mass (total specific internal energy) may then be calculated with:

$$e_{tot,s} = e_{t,s} + e_{rot,s} + e_{vib,s} + e_{exc,s} + e_{0,s} \tag{5}$$

The internal energy of a gas may be calculated by:

$$e = RT^2 \left(\frac{\partial \ln Q}{\partial T}\right)_V \tag{6}$$

Q represents the partition function, that describes the statistical properties of a system in thermodynamic equilibrium [1], and is given by:

$$Q = \sum_j g_j e^{\frac{-\varepsilon_j}{k_B T}} \tag{7}$$

Partitions functions are of particular importance since most thermodynamic properties of a system can be expressed using the partition function or its derivatives:

$$h = \sum_s c_s h_s \quad \text{with} \quad h_s = e_s + \frac{p_s}{\rho_s} = e_s + R_s T \tag{8}$$

$$C_v = \left(\frac{\partial e}{\partial T}\right)_v \quad \text{and} \quad C_p = \left(\frac{\partial h}{\partial T}\right)_p \tag{9}$$

$$C_p = T\left(\frac{\partial s}{\partial T}\right)_p \tag{10}$$

In this work, the thermodynamic properties are calculated using a polynomial model and thermodynamic database that describes them. The database previously used for air species was the Gordon and McBride database [22], which is limited to 20 000 K. However, the temperatures reached in this work surpass that limit, hence a updated database is required and will represent an important improvement for the modelling of hypervelocity flows. The process for obtaining this database, valid for temperatures up to 100 000 K, entails many steps.

An updated and thorough compilation of vibrational and rotational energies of the various neutral and ionized air species is therefore necessary to study hypersonic flows at high temperatures and represents one of the main accomplishments of this work. For atomic species, accurate level energy databases are available online [15] and one simply makes use of those energies. For diatomic species, experimental data is used to carry out the reconstruction of potential energy curves. This allows a better accuracy than any *ab initio* quantum method for determination of the potential.

The approach used in this work consists in potential curves' reconstruction, obtained using the RKR (Rydberg-Klein-Rees) method, that uses a set of experimental spectroscopic data for the part of curve of the energies from which these values were fitted from and then the RKR potential is extrapolated by a repulsive potential at shorter internuclear distances and by a Hulburt and Hirschfelder potential or a Extended Rydberg potential for longer distances. This method can be seen in more details in works such as [18] and represents advantages in rovibrational levels calculation over the Dunham expansion, as the latter's accuracy is strongly associated with the validity of the Dunham constants - obtained by fitting a specific set of measured rovibrational levels - which may yield inaccurate results outside of these limits. Furthermore, the range at which the constants were fitted is often not disclosed. So, it is more accurate to resort to numerical methods that reconstruct the state potential curve up to the dissociation limit and then determine the corresponding levels by solving the radial Schrödinger equation.

The process began with the compilation of spectroscopic data for the diatomic species considered, from multiple authors (such as [9, 16]), being given preference to experimental and more recent data. This was a laborious but essential task, as the database's usefulness is expected to translate to other areas that make use of spectroscopy, beyond the modelling of hypersonic high temperature flows, and to last for a long time, with future updates being made from this. In fact, and when compared to models and codes, databases' usefulness usually prevails in time.

For each molecule and for each of its electronic states here considered, a list is presented of their vibrational (ω_e, -$\omega_e x_e$, $\omega_e y_e$, $\omega_e z_e$, $\omega_e a_e$) and rotational constants (B_e, α_e, γ_e, δ_e), as well as the the minimum potential energy ($T(e)$), the dissociation products, the extrapolation potential used, the validity range of the spectroscopic constants and the references used.

The choice of extrapolation potential and v_{max} (when not available in literature) to be determined by the RKR potential was one that involved many trials and iterations. For each electronic level, possible errors were assessed, behaviour and interactions with other levels were analyzed and a conservative route was taken when not enough information was available, by reducing v_{max} or even limiting the reconstruction of the curve to the near equilibrium RKR part.

Figure 1 represents the potential curves for the O_2 states reconstructed in this work.

Comparison with other literature values [7, 16] showed that for most states there is an overall agreement. Nevertheless, differences were encountered and studied. More recent spectroscopic data, better reconstruction models, newly represented electronic states and different approaches dealing with perturbations that would impact the curves are the main causes for these differences

With all the potential curves reconstructed for the air molecular species in consideration, their energy levels were determined through the solution of the radial Schrödinger equation. Comparison of maximum numbers of vibrational and rotational levels with other literature allowed for further validations.

Finally, with all the energy levels calculated, the thermodynamic properties can be obtained, through the determination of the partition functions. This process is repeated for multiple values of temperature and the values obtained are then fitted using the expressions of Gordon and McBride [22]. The coefficients for those equations yield the updated thermodynamic database valid up to 100 000 K.

To compare and validate the obtained results, en-

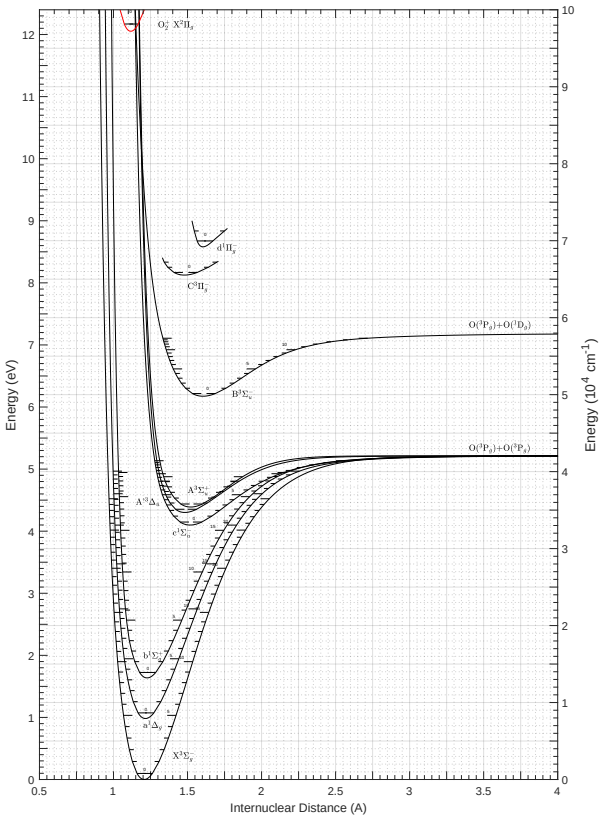

Figure 1: Potential curves for O_2 states.

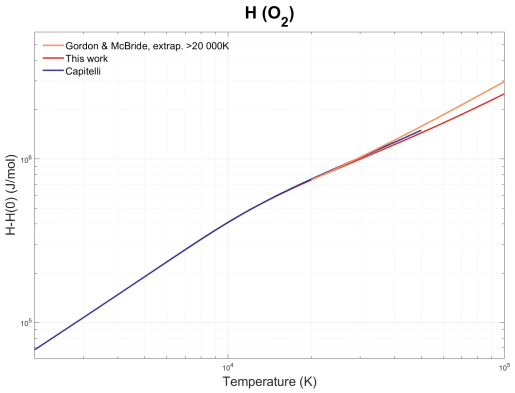

Figure 2: Enthalpy of O_2.

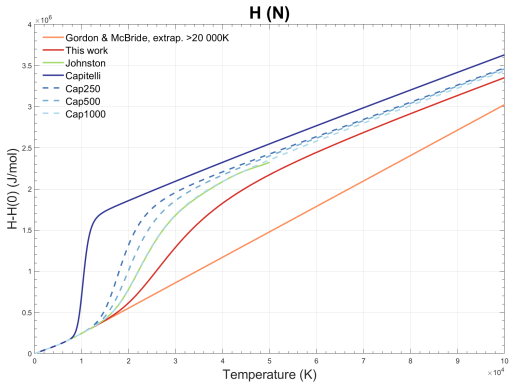

Figure 3: Enthalpy of N.

thalpy in function of temperature (H-H(0) (J/mol) vs T (K)) was plotted for the molecular species, using both the thermodynamics fits developed here and the ones by Gordon and McBride. These last ones were extrapolated for temperatures higher than 20 000K, by assuming a fixed slope. Additionally, a comparison was drawn with the thermodynamic properties determined by Capitelli [4] (up to 50 000 K).

Figure 2 presents the results for O_2. One may observe that for low temperatures the curves of this work and of Gordon and McBride are coincident, a good sign that the updated values are correct, as for low temperatures the lower lying energy levels will be the ones most populated and the Gordon and McBride coefficients already considered these energies. For the higher temperatures, the curves distance themselves, showing the importance of the updating of energies, as the simple extrapolations of the default values would lead to different results, overestimating them.

Comparison between the curves of this work and the ones by Capitelli show similarities in the trends, which validate the implementation of our new database. The differences in the values of both curves are a result of the different considered states (with this work presenting a more update set of states) and the fact that Capitelli uses spectroscopic constants beyond their validity limits.

For the atoms and their respective ions, the same comparison was made, but other data was also included: the curves using the coefficients determined by Johnston [10]. This work updated the thermodynamics fits for temperatures up to 50 000 K.

Figure 3 shows the enthalpy vs temperatures plots for N, with a linear scale to observe the differences at temperatures higher than 10 000 K in more detail.

As it was the case for molecules, there is here good agreement between the curves of the Gordon and McBride database and the updated one at lower temperatures. Likewise, for higher temperatures the updated curve differs from the extrapolated old one.

For N, the energy values by Johnston are different at higher temperatures. This occurs as we only consider the levels from NIST database, whereas Johnston accounts for additional higher-lying levels [11]. Interestingly, for N, the curve by Johnston agrees closely with the curve from Capitelli with ionization potential lowering of 1000 cm^{-1}, where additional Rydberg states are also accounted for.

For the ions of N, this difference is reduced.

Capitelli's polynomial fits differ from those developed in this work in the set of levels inserted in the partition functions, with [4] considering many more levels, as it uses extrapolation laws to include not observed Rydberg levels. This may lead to inaccurate thermodynamic properties, so ionization potential lowering should be considered. The properties using different ionization potential lowering values were also plotted. These still overestimate the enthalpy values when compared to the fits calculated in this work. Hence, for future updates of the database here developed, some additional Rydberg states may be also accounted for, providing that the adequate ionization potential lowering is being accounted for.

4.2. Chemical Kinetics

At high temperatures, chemical non-equilibrium conditions are encountered since equilibrium takes some time to be restored after the shock wave. This leads to the necessity of focusing on mass conservation for each species of the mixture, which was already included as additional equations (see equation 1). The source term in the mass conservation equation is modeled according to the relation expressing the net rate resulting from the forward and backward reactions. The forward rate may be estimated from the Arrhenius equation and the backward rate is obtained from the equilibrium constant $K_{eq,r}$.

This work makes use of three mixtures: one including 11 species (N_2, O_2, NO, N_2^+, O_2^+, NO^+, N, O, N^+, O^+, e^-), one with 13 (the previous ones plus N^{++}, O^{++}) and one with 15 species (the previous ones plus N^{+++}, O^{+++}).

For the 11 species mixture, different kinetic schemes may be considered. The reactions used in this work are the ones considered by [13] and include dissociation reactions, neutral exchange, associative ionization, charge exchange reactions and electron-impact ionizations reactions.

For the velocities and resulting temperatures considered in this work, further ionizations need to be included in the model, so more accurate results are obtained for the conditions where first ionization is capped.

The electron impact ionization rates used in this work for N^+ and O^+ to produce N^{++} and O^{++} respectively, are the ones determined by [10] from non-Boltzmann models for the production of N^{++} and assumption of equal equilibrium constant and recombination rate for O^{++}. As for the electron impact ionization rates of N^{++} and O^{++}, these were determined considering the ionization cross-sections from [2] to achieve a first reasonable estimate of the corresponding ionization rates.

The chemical reactions involving these double and triple ions are presented in table 1, with the constants to calculate the forward rates (with units of $m^3 mol^{-1} s^{-1}$).

Table 1: Chemical kinetics for double and triple ionized species.

Reaction	A	n	$\theta_R(K)$
$N^+ + e^- \rightleftharpoons N^{++} + e^- + e^-$	6.04E+06	0.603	341356
$O^+ + e^- \rightleftharpoons O^{++} + e^- + e^-$	6.90E+08	0.206	405511
$N^{++} + e^- \rightleftharpoons N^{+++} + e^- + e^-$	5.14E+06	0.588	550457
$O^{++} + e^- \rightleftharpoons O^{+++} + e^- + e^-$	2.17E+09	0.075	635568

4.3. Transport Properties

In this work, the Gupta-Yos transport model [8] is used, with a correction for ambipolar diffusion. The model relies on a simplification of the Chapman-Enskog solution and yields the transport properties by using an approximate mixing rule. This simplification consists on an averaging of the interactions between particles of different species; it takes into account the cross-section for each collision in the multi-component gas mixture, making it more accurate than the Wilke/Blottner/Eucken model, that considers this cross-section to be constant to all interactions. The Wilke model diverges from the exact solution for the high temperatures conditions considered in this work [21].

Since [8] does not provide information regarding the transport properties for N^{++}, O^{++}, N^{+++} and O^{+++}, these species' transport properties will be assumed equal to the values for their corresponding single ions [10], as their interactions with the gas species will be of the same nature.

It is noteworthy that the Gupta-Yos model starts to diverge from the real solution at higher temperatures as a result of higher ionization degrees. However, more accurate models, that considered fewer approximations, would be much more computationally expensive and have not been considered here.

5. Results

Simulations were performed to analyze the impact of the developed model improvements: the update of thermodynamic database and the inclusion of further ionizations. A 50 x 50 mesh around a spherical meteoroid (with radius of 0.3 m) was used, with adiabatic wall and refinement only at the shock wave. The simulations will have constant ram pressure of 0.1 MPa, a value chosen considering the typical conditions of first fragmentation of meteoroids in Earth's atmosphere, and various values of velocity will be simulated, in the 18-25km/s range.

5.1. Thermodynamic database influence

To compare the impact of thermodynamic database in the results, 11 species were considered in the gas mixture, as the Gordon and McBride (GM)

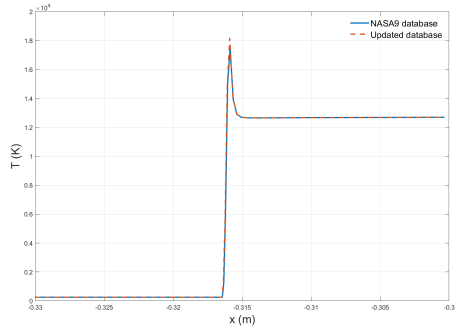

Figure 4: Stagnation line temperatures for simulations of 12 km/s using the NASA9 database vs the updated database.

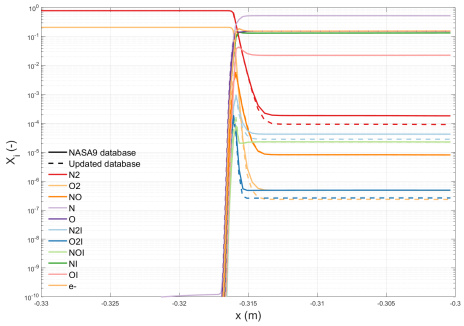

Figure 5: Stagnation line chemical species mole fractions for simulations of 12 km/s using the NASA9 database vs the updated database.

database does not include double and triple ions.

Evaluating the results of a simulation with 12 km/s (figures 4 and 5) shows that the curves using the Gordon and McBride (NASA9) database and the thermodynamic database developed in this work give coincident results. This was expected, as the temperatures do not surpass the 20 000 K mark and for these ranges the thermodynamic properties given by the two models are very similar. Dissociation and ionization phenomena may be observed in the plot of chemical species fractions at the stagnation line. One may also observe the existence of a plateau of constant properties, due to a quasi-steady-state being reached.

The main advantage of this work's extension of the thermodynamic database is actually the possibility of simulating the conditions with associated temperatures higher than 20 000 K (what would happen at velocities higher than 14 km/s, for p_{ram}=0.1 MPa), something that could not be done while using the Gordon and McBride database. When using the updated database the simulations converged to the expected results with no issues.

A comparison between simulations of 12 and

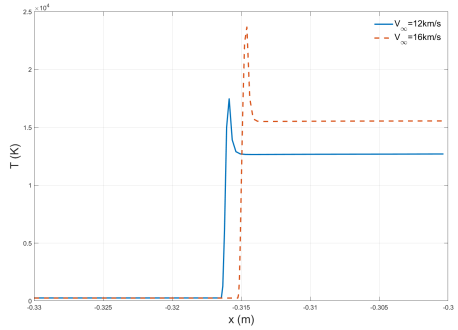

Figure 6: Stagnation line temperatures for simulations of 12 km/s vs 16 km/s, using the updated database.

16 km/s, both using the improved thermodynamic database are presented in figure 6. One may observe that the higher velocity simulation has a maximum temperature of approximately 23 680 K. Here, compared to the 12 km/s simulation, the temperatures reached for the 16 km/s are higher, as would be expected. Moreover, the shock is closer to the wall, which is also in concordance with the theory that, in general, higher velocities will translate to lower detachment shock distances [1]. For the 16 km/s simulation, the energy associated to the shock will be higher than for 12 km/s and a part of it will be transferred to the gas internal energy through chemical reactions, which naturally translates in higher degrees of ionization (with the concentration of electrons at 38 % approximately), as expected.

Moreover, a study regarding the impact of updating all species instead of only the atomic ones was performed. The difference in the stagnation line plots is small, as only a few cells in the shock have molecular species at high temperatures before they dissociate rapidly. Nevertheless, the effect of updating the molecules as well is felt in the stability of the numerical model, with the simulations with all species updated converging in less time than the simulations with only atomic species updated.

One may then conclude that the use of the updated thermodynamic database, although it does not represent a relevant change for temperatures lower than 20 000 K, is essential for simulations that reach higher temperatures.

5.2. Kinetic chemistry model influence

Now that the use of the updated thermodynamic database allows for higher velocity simulations, one may study the need for inclusion of further ionizations and its impact. Only the species that may impact the flowfield properties more significantly, by changing the chemical model, will be plotted in these graphs, to facilitate interpretation.

For velocities up to 18 km/s and considering a

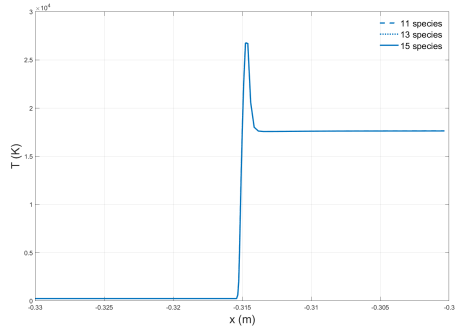

Figure 7: Stagnation line temperatures for simulations of 18 km/s, using the 11 vs 13 vs 15 species.

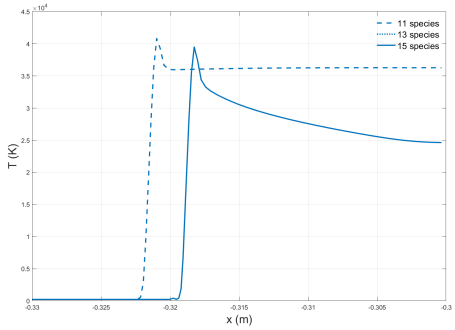

Figure 9: Stagnation line temperatures for simulations of 22 km/s, using the 11 vs 13 vs 15 species.

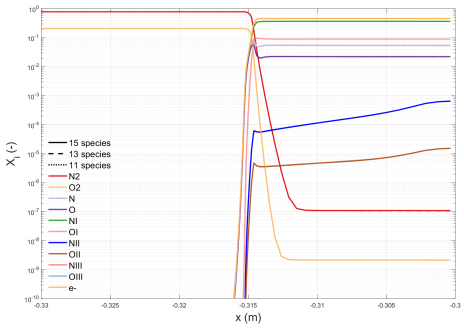

Figure 8: Stagnation line chemical species mole fractions for simulations of 18 km/s, using the 11 vs 13 vs 15 species.

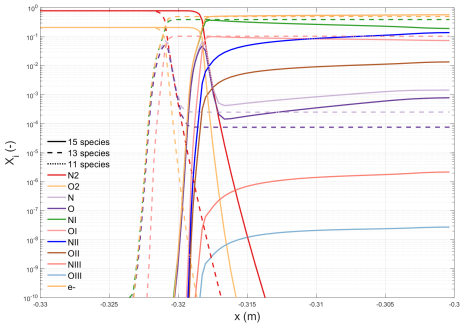

Figure 10: Stagnation line chemical species mole fractions for simulations of 18 km/s, using the 11 vs 13 vs 15 species.

gas mixture that allows for only first ionization (11 species gas mixture), it is possible to observe that the maximum concentration of electrons is below 46%. This means that first ionization is yet not capped and the inclusion of double and triple ionization would not have a relevant impact in the results. This may be observed in figures 7 and 8, with the plots using 11, 13 and 15 species presenting coincident results. The molar fractions plots for N^{+++} and O^{+++} are not presented in the figure as the concentrations are too low. Similar behaviour is verified for the simulations performed with velocities in the range of 8 km/s to 16 km/s.

However, as velocity increases, so do the energies involved and more and more ionization occur. For a velocity of 20 km/s or higher, one may observe that, with 11 species in the mixture, ionization is capped: the concentration of electrons is approximately 50% and the concentrations of remaining N and O to be ionized are negligible, so no extra energy may be transferred to the gas internal energy through further ionizations. This cap will lead to unrealistically high temperatures in the shock layer for higher velocity flows, as the extra energy of the shock wave will be transferred to translational temperatures higher than those encountered in simulations with 13 and 15 species.

In reality, double ionization will occur and the correspondent temperatures reached for each velocity case are lower. When 13 species gas mixture is considered, then the endothermic reactions of ionizing N^+ and O^+ into N^{++} and O^{++} represent another energy loss term that will decrease the temperatures in the shock layer. Double ionization is then necessary to be accounted for.

In figures 9 and 10, one may observe the difference in the results using gas mixtures with 11, 13 and 15 species, for a velocity of 22 km/s. Here, the inclusion of the double ionization decreases the maximum temperature from 40 840 K with 11 species to 39 470 K with 13, as the concentration of electrons changes from the capped value of 49.9% to 57%.

It is noteworthy that, contrarily to what was verified until 18 km/s and considering double ionization, at these conditions a quasi-steady-state plateau is not reached after the shock, with the temperature decreasing to 24 640 K at the wall, as the molar concentration of N^{++} increases up to 14%. This happens as double ionization rates are slower,

with the molar concentrations changing as reactions occur. For the case of 11 species, temperature after the shock remains at approximately 36 290 K.

Figures 9 and 10 present an important result, as one may observe that, in fact, the exclusion of relevant processes such as double ionization at this velocity, will significantly over-predict the temperatures in the shock layer, whilst the consideration of said processes will add important energy loss terms that approximate the results to what is expected to happen in reality. Additionally, the shock distance is smaller for the case of 13 species: since the conditions upstream of the shock are the same for both simulations, the pressure after the shock should be the same. Therefore, since the temperatures are lower for the 13 species case, then density needs to be greater and the shock moves closer to the wall.

Although double ionization is yet not capped for these conditions, simulations with 15 species are also included in the figures. The inclusion of triple ionization does not impact the temperature at the stagnation line, with the plot of the 15 species gas mixture coinciding with the one of 13. Nevertheless, this inclusion of further ionization increases simulation fidelity.

Simulations using a refined mesh, the new thermodynamic database and 15 species were performed until 25 km/s, where the maximum temperature is 49 200 K, then decreasing until 27 950 K at the wall, with a maximum molar concentration of electrons of 64%. At this velocity conditions, the molar fraction of N^{+++} and O^{+++} is approximately 7×10^{-5} and 2×10^{-6}.

For higher velocities, the presence of N^{+++} and O^{+++} would impact the results as the ionization of N^{++} and O^{++} would represent an important energy loss term for those conditions. This is expected to be more evident for conditions of capped double ionization - when the electron concentration would reach approximately 66% and, with a gas mixture of only 13 species, no further ionizations are available so extra energy involved on the shock would translate into nonphysical higher temperatures. The possibility of third ionization would solve the problem and more closely represent reality, as one expects these reactions to use a part of the extra energy and, therefore, the temperatures in the shock layer to be lower. Unfortunately, due to constrictions in time, it was not possible to reach convergence for this extreme conditions simulations, a problem arising from the large encountered gradients.

The inclusion of N^{++}, O^{++}, N^{+++} and O^{+++} represents, as anticipated, an important enhancement.

6. Conclusions

The major achievement of this work is the simulation of entry velocity flows in Earth's atmosphere never previously reached using the SPARK CFD code. Without the enhancements performed and implemented in this work, aerothermodynamic simulations using this code were limited to velocities below 14 km/s (for a ram pressure of 0.1 MPa). The extension of the thermodynamic database for all the species considered here, allowed for simulations with higher velocities and temperatures.

We compiled an updated and thorough spectroscopic database for the molecules and respective ions of this work, that represents a helpful resource for studies in various areas. The reconstruction of the potential energy curves is also an important deliverable of this work. With the energy levels determined and compared to other works, the results were deemed satisfactory and were used for partition function calculations. The thermodynamic database that fits the thermodynamic properties here determined also represents an useful resource for studies to come.

It was observed that capped ionization conditions encountered at 20 km/s would lead to inaccurately high temperatures in the shock layer when only simple ionization was being accounted for. To solve this problem, N^{++}, O^{++}, N^{+++} and O^{+++} were included in the gas mixture. The inclusion of double ionization decreased the temperatures found in the shock layer and allowed for simulations up to 25 km/s. For these ranges, double ionization was still not capped and the inclusion of triple ionization does not impact the flowfield significantly. Nevertheless, the fact that triple ionization is already included in the models will facilitate the work of others to come that wish to continue simulating higher and higher velocities.

This work supports the statement that increasing velocity will activate increasingly important energy loss terms, and the exclusion of these phenomena in the simulations will over-predict the temperatures reached in the shock layer. With the enhancements performed here, more models are available and tested in the SPARK CFD code, so more extreme hypersonic high temperature conditions of meteoroids entering the Earth's atmosphere may be simulated, furthering our understanding of hypersonic high-temperature flows and paving the way for these velocities to be considered for future Space missions.

To continue and improve the work developed here, the inclusion of radiative loss effects is essential. This could be done firstly in a loosely-coupled approach. As radiation effects increase, the impact of coupling becomes more important and ideally the simulation would be done in a completely coupled way, with each iteration involving CFD and radiative computations. The expected impact of coupled radiation is a decrease in shock layer temperatures.

The transport model should be improved, so it becomes more accurate for the ionization levels here considered. Further studies regarding the rates of electron-impact ionization reactions used could also be performed. As for the thermodynamic properties, fine-structure may be added to the set of levels considered for atomic species, adding more precision. The idea of adding some Rydberg levels to the set used should also be furthered and the inclusion of ionization potential lowering will represent an important feature.

Finally, more simulations using the models here developed should be performed, studying different conditions and continuously increasing the simulated velocities, extending the knowledge envelope for these fast flow regimes.

References

[1] J. D. Anderson Jr. *Hypersonic and High-Temperature Gas Dynamics, Second Edition*. 2006.

[2] K. L. Bell, H. B. Gilbody, J. G. Hughes, A. E. Kingston, and F. J. Smith. Recommended data on the electron impact ionization of light atoms and ions. *Journal of Physical and Chemical Reference Data*, 12(4):891–916, 1983.

[3] G. A. Bird. Approach to Translational Equilibrium in a Rigid Sphere Gas. *Physics of Fluids*, 6(10):1518–1519, Oct. 1963.

[4] M. Capitelli, G. Colonna, D. Giordano, L. Marraffa, A. Casavola, P. Minelli, D. Pagano, L. Pietanza, F. Taccogna, and B. Warmbein. Tables of internal partition functions and thermodynamic properties of high-temperature Mars-atmosphere species from 50K to 50000K. *ESA Scientific Technical Review*, 246, 09 2005.

[5] Z. Ceplecha and D. Revelle. Fragmentation model of meteoroid motion, mass loss, and radiation in the atmosphere. *Meteoritics Planetary Science*, 40:35 – 54, 01 2005.

[6] J. Coelho. Aerothermodynamic Analysis of Aerocapture and Ballistic Entry Flows in Neptune's Atmosphere. Master's thesis, Instituto Superior Técnico, December 2020.

[7] F. Gilmore. Potential energy curves for N2, NO, O2 and corresponding ions. *Journal of Quantitative Spectroscopy and Radiative Transfer*, 5(2):369–389, Apr. 1965.

[8] R. Gupta, J. Yos, R. Thompson, and K.-P. Lee. A review of reaction rates and thermodynamic and transport properties for an 11-species air model for chemical and thermal nonequilibrium calculations to 30000 K. 09 1990.

[9] K. P. Huber and G. Herzberg. *Constants of diatomic molecules*, pages 8–689. Springer US, Boston, MA, 1979.

[10] C. Johnston and A. Brandis. Aerothermodynamic Characteristics of 16-22 km/s Earth Entry. 06 2015.

[11] C. Johnston, B. Hollis, and K. Sutton. Spectrum Modeling for Air Shock-Layer Radiation at Lunar-Return Conditions. *Journal of Spacecraft and Rockets - J SPACECRAFT ROCKET*, 45:865–878, 09 2008.

[12] C. Johnston and E. Stern. A Model for Thermal Radiation from the Tunguska Airburst. *Icarus*, 327, 02 2019.

[13] C. O. Johnston and M. Panesi. Impact of state-specific flowfield modeling on atomic nitrogen radiation. *Phys. Rev. Fluids*, 3:013402, Jan 2018.

[14] C. O. Johnston, E. C. Stern, and L. F. Wheeler. Radiative heating of large meteoroids during atmospheric entry. *Icarus*, 309:25–44, 2018.

[15] R. Y. R. J. Kramida, A. and N. A. Team. NIST Atomic Spectra Database (version 5.9), [Online]. Available: https://physics.nist.gov/asd [Wed Apr 20 2022]. National Institute of Standards and Technology, Gaithersburg, MD, 2021.

[16] P. H. Krupenie. The Spectrum of Molecular Oxygen. *Journal of Physical and Chemical Reference Data*, 1(2):423–534, 1972.

[17] M. Lino da Silva. *Simulation des propriétés radiatives du plasma entourant un véhicule traversant une atmosphére planétaire á vitesse hypersonique: application á la planéte Mars*. PhD thesis, Université d'Orléans, France, 2004.

[18] M. Lino da Silva, V. Guerra, J. Loureiro, and P. Sá. Vibrational distributions in N2 with an improved calculation of energy levels using the RKR method. *Chemical Physics*, 348:187–194, 06 2008.

[19] M. Lino da Silva, J. Loureiro, and V. Guerra. Rotational nonequilibrium in state-resolved models for shock-heated flows. *Chemical Physics*, 398:96–103, 2012. Chemical Physics of Low-Temperature Plasmas (in honour of Prof Mario Capitelli).

[20] B. Lopez and M. Lino Da Silva. *SPARK: A Software Package for Aerodynamics, Radiation and Kinetics*.

[21] D. D. Loureiro. High-Temperature Modeling of Transport Properties in Hypersonic Flows. Master's thesis, Instituto Superior Técnico, November 2015.

[22] B. McBride, M. Zehe, and S. Gordon. NASA Glenn coefficients for calculating thermodynamic properties of individual species. 10 2002.

[23] O. Popova. *Meteoroid Ablation Models*, volume 95, pages 303–319. 08 2006.

[24] E. A. Silber, M. Boslough, W. K. Hocking, M. Gritsevich, and R. W. Whitaker. Physics of meteor generated shock waves in the Earth's atmosphere – A review. *Advances in Space Research*, 62(3):489–532, 2018.

[25] J.-k. Wang and Z.-s. Wu. Improved Calculation of Vibrational Energy Levels in F2 Molecule using the RKR Method. *Chinese Journal of Chemical Physics*, 23(2):155–159, 2010.